frontiers in Physics

ORIGINAL RESEARCH
published: 29 October 2020
doi: 10.3389/fphy.2020.592875

Exploiting Cross-Luminescence in BaF_2 for Ultrafast Timing Applications Using Deep-Ultraviolet Sensitive HPK Silicon Photomultipliers

Rosalinde Hendrika Pots[1,2]*, *Etiennette Auffray*[1] and *Stefan Gundacker*[1,3]

[1] The European Organization for Nuclear Research (CERN), Meyrin, Switzerland, [2] Fakultät 1, Rheinisch-Westfälische Technische Hochschule Aachen, Aachen, Germany, [3] Dipartimento di Fisica "Giuseppe Occhialini", Universitá degli studi di Milano Bicocca, Milano, Italy

Time resolution of scintillation-based detectors is becoming continuously more important, both for medical applications, especially in positron emission tomography (PET), and in high energy physics. This article is an initial study on exploiting the fast cross-luminescence emission in the inorganic BaF_2 scintillator with deep ultraviolet-sensitive silicon photomultipliers (SiPMs) from Hamamatsu for precise timing in PET and HEP. Using small BaF_2 pixels optimized for timing read out by these photodetectors with a photon detection efficiency (PDE) of only about 15% in the desired 200 nm emission region, a coincidence time resolution (CTR) of 94 ± 5 ps full width at half maximum (FWHM) is achieved when coupling with air. This figure improves to 78 ± 4 ps FWHM when coupling the BaF_2 crystal with UV transparent optical grease, Viscasil, to the photodetector. This CTR performance obtained with BaF_2 is better than that measured with LYSO:Ce, a commonly used state-of-the-art inorganic scintillator in PET, when coupled to another Hamamatsu photodetector (S13360), having a PDE of 60% at 420 nm, with Meltmount. In view of the prospects in advancing technologies for ultraviolet sensitive SiPMs, with high PDE and single photon time resolution, and further advancements in producing high quality BaF_2, one could imagine the development of sub-30 ps FWHM time-of-flight-PET systems.

Keywords: coincidence time resolution, scintillator, cross-luminescence, silicon photomultiplier, deep ultraviolet, positron emission tomography, high energy physics, BaF_2

OPEN ACCESS

Edited by:
Paul Sellin,
University of Surrey, United Kingdom

Reviewed by:
Yadong Xu,
Northwestern Polytechnical University, China
Lodovico Ratti,
University of Pavia, Italy

***Correspondence:**
Rosalinde Hendrika Pots
rosalinde.hendrika.pots@cern.ch

Specialty section:
This article was submitted to Radiation Detectors and Imaging, a section of the journal Frontiers in Physics

Received: *08 August 2020*
Accepted: *22 September 2020*
Published: *29 October 2020*

Citation:
Pots RH, Auffray E and Gundacker S (2020) Exploiting Cross-Luminescence in BaF_2 for Ultrafast Timing Applications Using Deep-Ultraviolet Sensitive HPK Silicon Photomultipliers. Front. Phys. 8:592875. doi: 10.3389/fphy.2020.592875

1. INTRODUCTION

Scintillating crystals are widely used for the detection of ionizing particles and gamma radiation in various applications, e.g., in high energy physics and medical imaging, where high time resolution plays an ever more significant role. In medical applications, especially in positron emission tomography (PET), the precise time-of-flight (TOF) information would lead to higher signal-to-noise ratio imaging, thus allowing to reduce the administered radioactive dose to the patient and/or the scanning time. High-luminosity particle physics experiments would benefit from high resolution timing in order to cope with serious pile-up effects, especially important in the search for rare events and new physics.

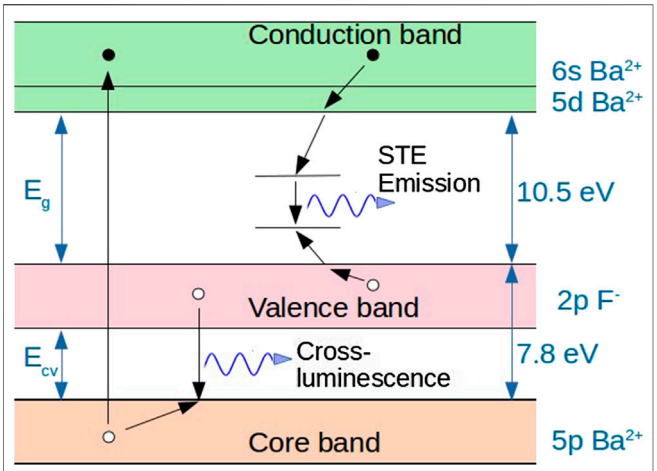

FIGURE 1 | Schematic overview of the band-gap diagram of BaF_2 and corresponding emission mechanisms, based on ref. [15].

For this purpose, there is a large effort in many groups focusing on inorganic scintillators for the improvement of time resolution [1–10],[1,2] for instance by exploiting intrinsically fast scintillation processes with short rise- and decay times. Due to its fast cross-luminescence emission, BaF_2 is an excellent candidate in this perspective.

Since the beginning of the 1970s, it is known that BaF_2 is a scintillator exhibiting self-trapped exciton (STE) emission between the conduction and valence band. This is the slow emission at 320 nm, with a decay time (τ_d) of 630 ns [11].

More than 10 years later, a second emission band at 220 nm was discovered [12]. It has been established that, on top of the self-trapped exciton emission at 320 nm, BaF_2 has two main emission peaks at 220 and 195 nm, with a shoulder at ~175 nm [13], originating from cross-luminescence, with a sub-nanosecond decay time. This decay time was measured to be only 0.6 ns [14], making BaF_2 the fastest inorganic scintillator at the time [15].

Cross-luminescence emission is a scintillation process where an electron is excited from the core band to the conduction band. The resulting hole in the core band then recombines with an electron in the valence band. This process is illustrated in **Figure 1**. Since the valence band contrary to the conduction band, is filled with electrons with which the hole in the core-band can recombine, the recombination probability is large. As such, cross-luminescence is an intrinsically fast scintillation process resulting in a very short light pulse with a typical decay time of the order of nanoseconds or less.

Cross-luminescence is also referred to as core-valence luminescence [16, 17] and Auger-free luminescence [18]. Cross-luminescence is only exhibited by crystals that have a band gap between the valence band and the top of the core band with an energy difference E_{cv} of less than the energy difference E_g between the conduction and valence band [15–19], the forbidden band gap that is usually involved in the scintillation process.

BaF_2 is not the sole cross-luminescent material known, yet it is among the fastest ones and, with a reported light yield of 1,400 ph/MeV for the fast emission, also one of the brightest ones [19]. Furthermore, it is not hygroscopic, unlike for example CsF. Therefore, after its discovery there has been an enormous interest in BaF_2, and numerous research groups started investigating this material [5, 12, 14, 20–24], both to understand its characteristics and to use it in detectors incorporating time-of-flight information. **Table 1** shows an overview of the characteristics of BaF_2, as well as those for LYSO and BGO for comparison.

Owing to its favorable timing characteristics, as also shown in **Table 1**, BaF_2 has been a center of interest since the early eighties of the last century [14, 16, 17, 30, 31]. However, the difficulty with cross-luminescence is that the emission is in the deep UV. For this reason, it was not possible to fully benefit from the timing potential in the past with photodetectors available at that time. However, recent developments in solid state photodetectors with internal gain for experiments using liquid xenon as scintillating material lead to the necessity of measuring light at the very short wavelength of 175 nm [32, 33]. This has recently also made new aspects of exploiting cross-luminescence feasible.

Comparing the properties of BaF_2 with LYSO:Ce, a state-of-the-art crystal widely used in time-of-flight PET scanners, a rough estimate of its potential can be made using the following relation for its coincidence time resolution (CTR) as a function of decay time and light yield: $CTR \propto \sqrt{\tau_d / LY}$. Considering that LYSO:Ce has a light yield of 40 kph/MeV and a decay time of about τ = 39 ns [10], and that BaF_2 has a reported light yield (of the fast emission) of only 1,400 ph/MeV but with a decay time of 0.6–0.8 ns [22], this immediately leads to a CTR performance superior by a factor of 1.3–1.5 over that of LYSO:Ce. This consideration is based on the assumption of using a photodetector with a similar PDE in the deep UV as at 420 nm.

This promising potential in CTR performance, considering also the relatively low production cost of BaF_2 [29], makes this crystal all together promising for our investigation.

This paper summarizes initial investigations on the timing potential of cross-luminescence in BaF_2 using current state-of-the-art technology. The results of the CTR measurements using SiPMs of Hamamatsu, especially developed for measurements in the deep UV, will be presented in this work. Furthermore, the effect of optical coupling greases on the light extraction and the CTR has been evaluated. This may reignite new interest for further research on BaF_2.

2. MATERIALS AND METHODS

2.1. Crystal Samples

In the study presented in this article, BaF_2 samples from two different producers were used: Epic Crystals[3], and Proteus[4]. All

[1]Project description of the Fast Cost Action: https://www.cost.eu/actions/TD1401/, accessed July 18, 2020.

[2]Home page of the 10 ps challenge: https://the10ps-challenge.org/, accessed July 18, 2020.

[3]Homepage Epic Crystals: http://www.epic-crystal.com/, accessed July 13, 2020.

[4]Homepage Proteus Crystals: https://proteus-pp.com/, accessed July 13, 2020.

TABLE 1 | Overview of the general characteristics of BaF_2, LYSO, and BGO. Values are taken from the book Inorganic Scintillators for Detector Systems [19], unless otherwise indicated.

	BaF_2	LYSO	BGO
Density ρ (g/cm^3)	4.88	7.4	7.13
Z_{eff}	53	66	75.2
Photon absorption coefficient α @ 511 KeV (cm^{-1})	0.085	0.28	0.336
Radiation length X_0 (cm)	2	1.1	1.12
LY_{intr} (ph/MeV)	1,400[a] [22] 9,500[b] [22]	40,000	10,000 [10]
Decay time τ (ns)	0.6 – 0.8[a] 620[b]	40	300
Photon fraction @ 0.5 MeV	0.19 [25]	0.34 [25]	0.43 [25]
Emission peak(s) λ_{max} (nm)	195[a] 220[a] 310[b]	420 [10]	480 [10]
Refractive index (RI) @ λ_{mac}	1.56 [26] 1.55 [26] 1.50 [26]	1.82 [10]	2.1 [10]
Melting point ($^\circ C$)	1,280 [27]	2,150 [28]	1,050 [28]
Cost ($/$cm^3$)	15 [29]	60 [29]	35 [29]

[a]*Cross-luminescence.*
[b]*STE emission.*

samples are pure BaF_2 without any doping. From both producers, a crystal size of $2 \times 2 \times 3$ mm^3 was used. Shorter crystals are more suitable for comparing the timing performance of BaF_2 with other crystals as absorption and imperfection effects, more likely present in longer crystals, play less of a role.

2.2. Optical Coupling Greases

To optimize light extraction from the crystal, inorganic scintillators are generally coupled to a photodetector using an optical coupling agent. The difficulty here is that there are not many materials on the market that are transparent to UV-light with wavelengths below 250–300 nm. Previously Klamra et al. [31] and Zhu [34] have reported their research on this subject. This article presents a study on the suitability of some selected greases as optical coupling agents for BaF_2 and also for measurements in conjunction with the specific VUV SiPMs.

Rhodorsil 47V was one of the first greases tested in conjunction with BaF_2. Meltmount, which is a frequently used coupling agent (note: this coupling agent acts like a heat sensitive glue, allowing to remove pixels from the SiPM upon heating of the glue) in our lab, was also added to the test series, as well as Dow Corning 200 (500.000 cst) since it was deemed to be very transparent in the deep UV by Klamra et al. [31]. Further added to the measurements was Viscasil, also claimed to be very transparent in the deep UV and tested by Klamra et al. [31]. Finally, also glycerine was tested as a promising candidate. The difficulty with glycerine is that it behaves more like a liquid and is therefore more difficult to handle than the other greases since they are more viscous.

2.3. Silicon Photomultipliers

Common SiPMs on the market are not compatible with light emitted in the deep UV. There are several reasons for this [35]. One apparent reason is that, in order to protect the wire bonds of the SiPM and the sensor itself, a protection layer is applied on top of the SiPM [35], usually made of glass or epoxy. Both are not transparent to deep UV light. Underneath the protection layer is usually an anti-reflective layer, which is not designed for UV light either.

Furthermore, deep UV light with a wavelength of around 200 nm only penetrates a few nanometers into the silicon layer [35]. This is about 100 times shallower than for light above 400 nm. This has the effect that the electron-hole pairs are effectively created at the surface of the SiPM, making it difficult to retain high photon detection efficiencies (PDEs).

Therefore, in this work a SiPM specifically developed for measurements in the vacuum UV (VUV) was used, i.e., the Hamamatsu S13370-3050CN5 primarily developed for dark matter searches with liquid xenon. This SiPM then does not possess a layer to protect the wire bonds, nor to protect its surface, making it fragile and prone to damage when applying greases on its surface.

According to its datasheet, this SiPM has a photon detection efficiency (PDE) of about 24%[5] at 175 nm and is constant up to at least 200 nm. An independent measurement, however, indicates a PDE of only $\sim$15% at 175 nm [33]. While the SiPM was measured to have a breakdown voltage of 51.5 $\pm$ 0.2 V, the regular comparative CTR measurements were run at 60 V (i.e., at an overvoltage of 8.5 V). A higher operating voltage of up to 61 V (i.e., an overvoltage of 9.5 V) was only used to exploit the CTR performance limits of the SiPM.

2.4. Characterization Methods

2.4.1. Transmission

Transmission measurements were performed with a Perkin Elmer LAMBDA 650 UV/VIS Spectrometer.[6] This device can

[5]Datasheet of HPK S13370-CN: https://www.hamamatsu.com/jp/en/product/optical-sensors/mppc/mppc_mppc-array/index.html, accessed January 28, 2019.
[6]Product description of the Perkin Elmer LAMBDA 650 UV/VIS Spectrometer: https://www.perkinelmer.com/lab-solutions/resources/docs/BRO_Lambda950850650Americas.pdf, accessed May 26, 2020.

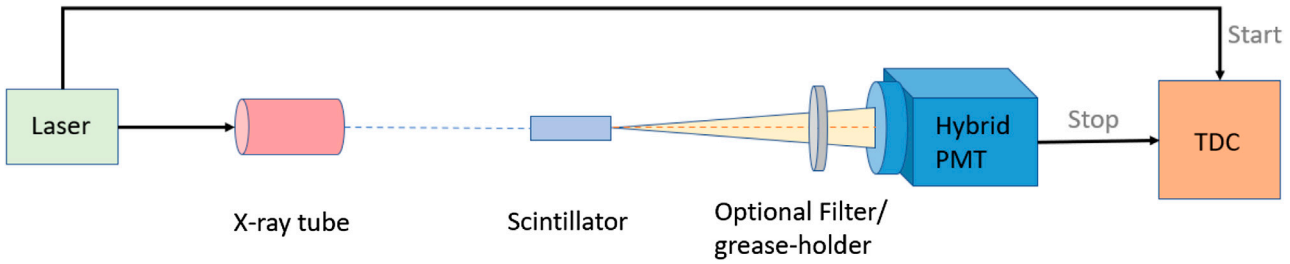

FIGURE 2 | Illustration of the time correlated single photon counting (TCSPC) setup, using an X-ray tube excited by a picosecond laser, hybrid-PMT, and a fast TDC. Filters can be placed in front of the hybrid-PMT.

measure transmission of samples using light with wavelengths between 190 and 900 nm. To measure the transmission of the viscous optical coupling agents, the grease under test was applied as a thin layer between two quartz plates, which had been tested beforehand to be transparent down to 190 nm. This is used to correct the later transmission measurements of the greases for the effect of Fresnel reflection.

2.4.2. Light Output

The light output is measured by exciting the scintillating crystal with a ^{137}Cs source emitting gammas with an energy of 662 keV. The generated light is collected by a VUV sensitive photomultiplier tube (PMT), a Hamamatsu H6610. The PMT signal is digitized and gives an energy spectrum with a Compton shoulder and a photopeak. The position of the photopeak defines the light yield of the crystal. In this study, the light output (LO) is mainly used to measure the gain of extracted light with respect to air as a function of the different coupling greases used. The amount of extracted light is measured relative to the known light output of an LYSO pixel (LO_{LYSO}), that is thus used as LO reference in this study. To do so, the extracted amount of light is calculated by:

$$LO = \frac{PPP_{BaF_2}}{PPP_{LYSO}} * \frac{QE_{LYSO}}{QE_{BaF_2}} * \frac{1}{LO_{LYSO}} \quad (1)$$

where PPP_{BaF_2} refers to the photopeak position for the BaF_2 crystal and QE_{BaF_2} to the effective quantum efficiency of the PMT for the emission spectrum of BaF_2. PPP_{LYSO} refers to the photopeak position of the LYSO pixel and QE_{LYSO} to the effective quantum efficiency of the PMT for LYSO emission.

2.4.3. Time Correlated Single Photon Counting

The time correlated single photon counting (TCSPC) measurements were performed with the setup illustrated in **Figure 2**. A Hamamatsu N5084 pulsed X-ray tube coupled to a picosecond laser with a FWHM of ~50 ps excites the crystal under test. At the same time the laser driver produces a start signal for the fast time-to-digital converter (Cronologic xTDC4). The light produced by the X-rays traversing the crystal is measured by a hybrid PMT HPM-100-07 from Becker & Hickl and provides the stop to the TDC. Every time a pulse is generated in the X-ray tube, a time measurement is started and the time delays of the detected single photon signals in the hybrid PMT recorded. In this way the scintillation pulse produced by the scintillator is basically sampled one photon at a time. A histogram of the delay times is produced, showing the full kinetics of the scintillation light. The impulse response function (IRF) of the entire setup was measured to be 162 ps FWHM and was taken into account in the data analysis (fit of the decay and rise times). The quantum efficiency of the hybrid PMT is only reported for values $\geq$220 nm, with a steep decline from 280 nm downwards. As a result, the abundance of light emitted in the deep UV could be underestimated.

To measure the grease-induced absorption for the different decay components, two plates of quartz with a thin layer of optical grease applied between them are placed between the BaF_2 crystal and the hybrid PMT. As such, the grease acts as a filter, and the measurement would only indicate a possible absorption by this grease on the light emitted by the BaF_2 crystal. It is important to notice that this measurement does not show the effect of increased light extraction provided by the higher refractive index of the optical greases compared to air-extraction.

2.4.4. Coincidence Time Resolution

The coincidence time resolution (CTR) is measured with the setup illustrated in **Figure 3**. In the setup two scintillators are facing each other in a back-to-back arrangement and are excited by two correlated and co-linear gammas of 511 keV originating from a ^{22}Na source placed between the two crystals. One of the two crystals is a LSO:Ce:0.2%Ca coupled with Meltmount to a FBK NUV-HD SiPM independently measured with a CTR_{ref} of 60 $\pm$ 3 ps FWHM [10]. The other is the BaF_2 crystal coupled to a Hamamatsu VUV S13370-3050CN SiPM. The measured coincidence time resolution of the total system, CTR_{tot}, is a combination of the time resolution of the BaF_2 and the reference crystal, where $CTR_{tot} = \sqrt{\frac{1}{2} \times (CTR_{ref}^2 + CTR_{BaF_2}^2)}$. Therefore, the time resolution of the BaF_2 crystal under investigation (CTR_{BaF_2}) is calculated as follows: $CTR_{BaF_2} = \sqrt{2 \cdot CTR_{tot}^2 - CTR_{ref}^2}$. Both the reference crystal and the BaF_2 crystal are coupled to a SiPM, from where the signal is split a) for time stamping with a high frequency amplifier with ~1.5 GHz bandwidth [8] and b) for an independent pulse height measurement with a low-noise analog operational amplifier [8], designed to obtain the energy of the photoelectric peak. The signals are digitized with a LeCroy DDA 735Zi oscilloscope. After selecting data solely originating from the photopeak (511 keV), the CTR is determined as the FWHM of the Gaussian fit to the histogram of the time delays.

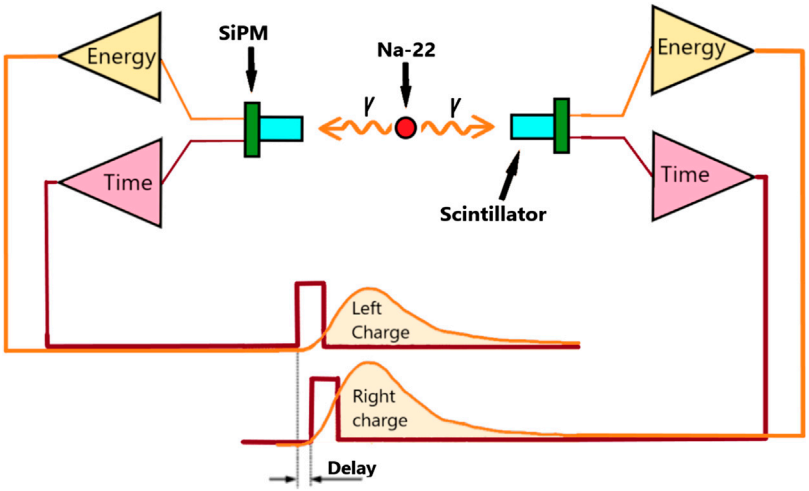

FIGURE 3 | Illustration of the coincidence time resolution (CTR) setup, based on ref. [8].

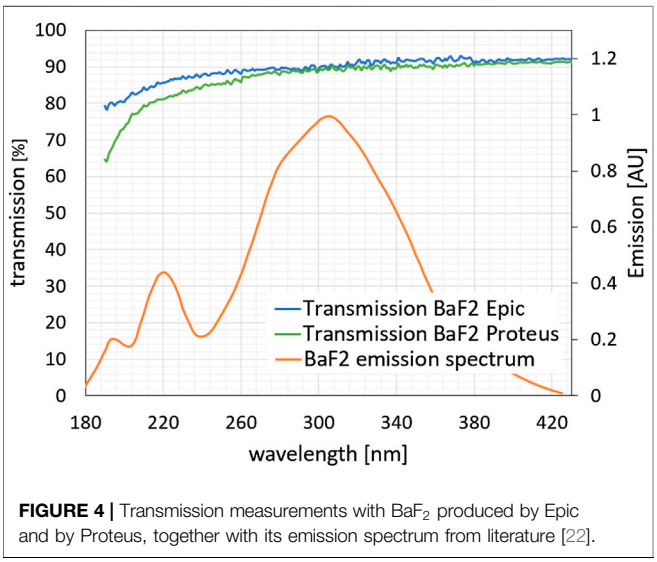

FIGURE 4 | Transmission measurements with BaF_2 produced by Epic and by Proteus, together with its emission spectrum from literature [22].

As mentioned before, the BaF_2 crystal is coupled to a Hamamatsu S13370-3050CN SiPM, specifically developed for the measurement of VUV light. This SiPM has a surface of 3×3 mm^2, enabling to position the BaF_2 with a smaller readout surface of 2×2 mm^2 such that it does not touch the wire bonds of the SiPM.

3. RESULTS

3.1. Transmission Measurements

To determine the transparency of the BaF_2 crystals for their own emission spectrum, the transmission of the samples of the two different producers have been measured. The results, as shown in **Figure 4**, indicate that both crystals are very transparent down to ~300 nm. Below that point, the Proteus crystal gradually absorbs light. The Epic crystal, on the other hand, continues to be very transparent down to ~270 nm, from where on it starts to absorb as well, however less steeply than the Proteus crystal. Therefore, the absorption is mainly in the domain of the fast cross-luminescence emission. Despite the shortness of the crystal, of only 3 mm, the effective photon path length before detection is significantly larger [36], such that the observed absorption along this path may have an effect on the CTR of the crystals.

Figure 5 shows the transmission of the measured greases. They show that Meltmount is clearly not suitable as a glue for BaF_2 and consequently was excluded from further tests. Rhodorsil also shows a significant absorption, with a center at around 250 nm and a cut-off at ~210 nm. It was therefore deemed unsuitable for further measurements with BaF_2 as well.

As to Dow Corning and Viscasil, the differences between the two of them are insignificant. Both are close to 100% transparent down to 220 nm, from where on they both start to absorb gradually. They both seem to have a cut-off at ~190 nm, also observed by Zhu [23] and Dorenbos et al. [22]. All together, Dow Corning 200 and Viscasil look suitable as optical coupling compounds for BaF_2 measurements.

In contrast to Dow Corning and Viscasil, glycerine extends its transparency even further down to shorter wavelength before it also rolls off.

3.2. Light Output Measurements

Table 2 gives an overview of the light output measurements with the greases that had been investigated, as well as the corresponding gain in light extraction compared to measurements with air coupling.

The light output from the Proteus crystal is consistently higher than that from the Epic crystal, on average by about a factor 1.15.

Table 2 further shows that all greases clearly improve light extraction from the crystals. Comparing the results from the three grease measurements with those obtained from air-coupling measurements, a gain in extracted light of 1.6–1.8 is observed for both crystals.

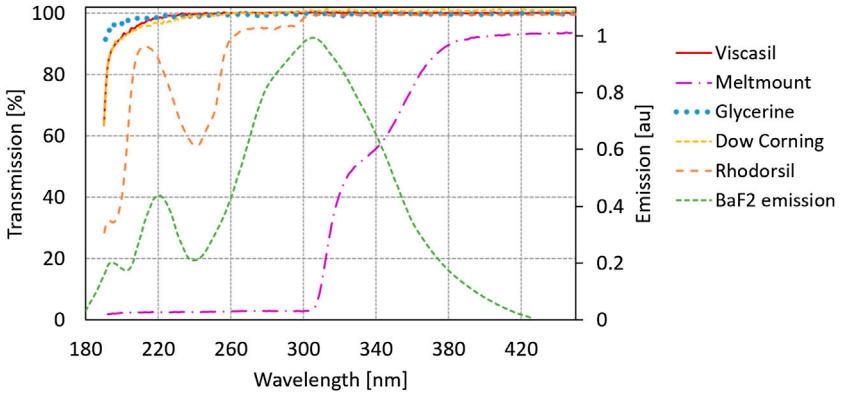

FIGURE 5 | Transmission measurements of several optical couplings agents between two quartz plates, performed between 190 and 440 nm, corrected for the absorption by one quartz plate and the Fresnel reflection between the quartz/air interfaces. Also the emission spectrum of BaF_2 has been plotted for comparison [22].

TABLE 2 | Light output measurements on 2 × 2 × 3 mm^3 BaF_2 crystals from Epic and Proteus, coupled to a Hamamatsu H6610 PMT with several optical coupling media and wrapped in several layers of Teflon. The error in the measurements is about 10%.

	Light output Epic (kph/MeV)	Gain w.r.t Air-coupling	Light output Proteus (kph/MeV)	Gain w.r.t Air-coupling
Air	2.9		3.7	
Viscasil	4.5	1.55	5.6	1.67
Dow corning	5.1	1.75	5.7	1.70
Glycerine	5.1	1.75	6.0	1.77

3.3. Time Correlated Single Photon Counting Measurements

In a first round, the kinetics of the BaF_2 emission of crystals from both Epic and Proteus were measured, with no greases used. The results are shown in **Figure 6**.

Since two decay channels were expected from literature, one for cross-luminescence and one for the STE emission, the data was initially fitted with a double exponential decay function. The results of these fits are shown in the left graphs of **Figure 6**. Notwithstanding its low χ^2 value, see **Table 3**, the double exponential decay function shows a deficiency with respect to the data-points in the first nanosecond of the emission, thus leading to the assumption that there is an additional, very fast, decay component in the emission spectrum. To test this hypothesis, the data was then fitted with a triple exponential decay fit, as shown in the graphs on the right-hand side of **Figure 6**. While the χ^2 improved marginally, the fit clearly follows better the data-points in the first nanosecond of the emission, thus indicating a better fit to the data. The results of the double exponential and triple exponential fits are summarized in **Table 3**. The measurements do reveal a third, very fast, decay component with a derived decay time of ~0.1 ns and an abundance of ~1% for both crystals.

As to the origin of the very fast decay component, some groups have claimed the existence of hot intraband-luminescence in BaF_2 [5, 24]. Considering that hot intraband-luminescence is emitted over the entire light spectrum, a measurement with a 400 nm longpass filter, placed between the crystal and the hybrid PMT, has been performed with the result that only noise showed up. This excludes the proclaimed hot intraband-luminescence as to the origin of the here observed very fast emission component. To investigate the very fast component further, this time a 250 nm longpass and a 240–395 nm bandpass filter have been used. From the 250 nm measurement only the two known decay components (0.6 and 600 ns) were observed, with the other very fast emission absent. From the measurement with the bandpass filter, reaching wavelengths below 250 nm yet limited to 240 nm, the very fast component showed up again, however with only half of its original abundance. This leads to the conclusion that at least the majority of the emission of the very fast decay component must be below 240 nm.

The measurements in **Figure 6** furthermore show that both crystals have a decay time of 0.7 ns for the component identified as the cross-luminescence emission, with an abundance of ~5%. The decay times of ~700 ns and ~600 ns for Epic and Proteus, respectively, both with an abundance of 94%, were identified as the STE emission. These values are comparable with literature values. The abundance of cross-luminescence emission is lower than expected from literature, which can be attributed to the lower detection efficiency in the deep UV of the hybrid-PMT used in this work. There is no difference in the observed abundance of cross-luminescence between the two crystals.

To investigate the effect of the chosen greases on the abundances of the different decay components, it was preferred to use the double exponential decay function for the fitting of the data, thus determining an effective decay time and abundance for the two fast components together. A fit with three decay components would have resulted in a sharing of the statistics of the emission over two more fitting parameters, thus reducing the statistics per parameter such that too many statistical fluctuations are introduced. These fluctuations will affect the fitted values for the abundances and decay times of both the very fast component and the cross-luminescence.

Table 4 shows the results of the measurements with the selected optical coupling greases, fitted with a double exponential decay function. The fits indicate that the fast

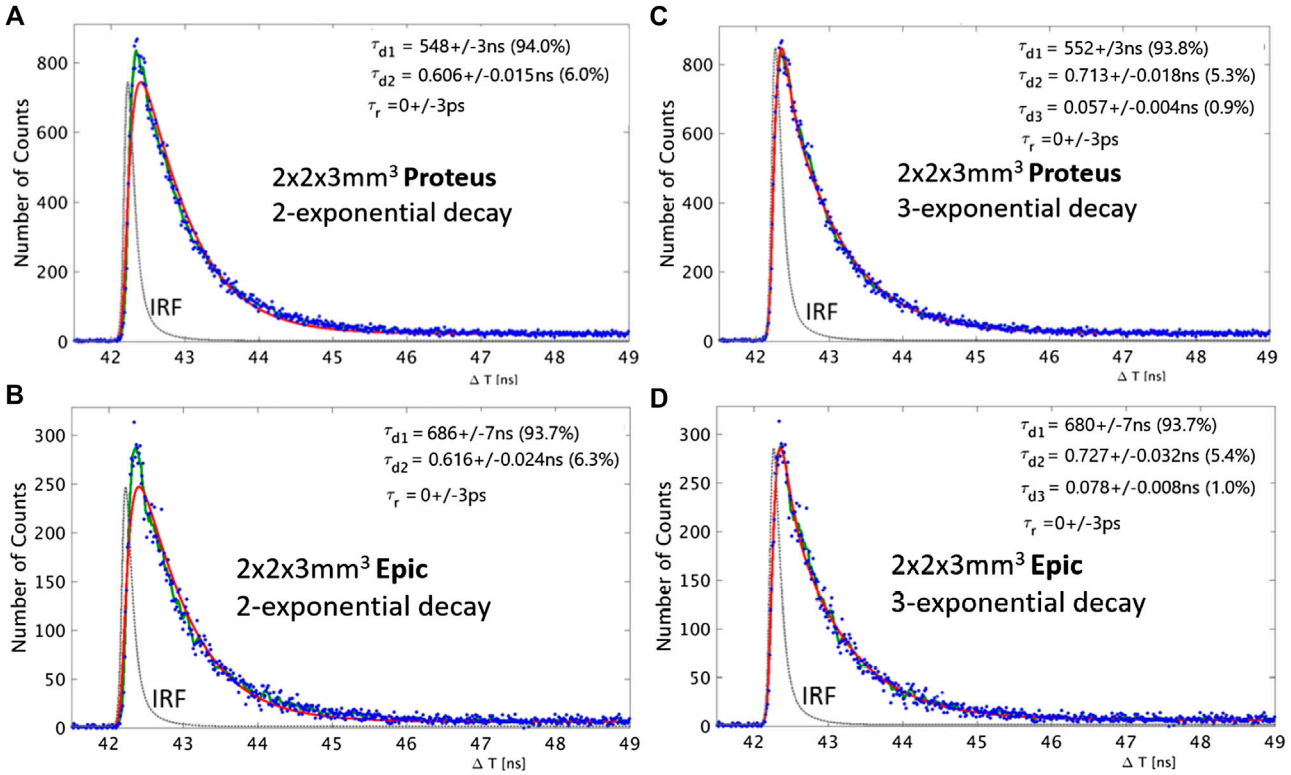

FIGURE 6 | Time correlated single photon counting measurements under X-ray excitation, with 3 mm long BaF_2 crystals from Proteus **(A, C)** and Epic **(B, D)**, measured with a gate of 2 μs. The thin black dotted line shows the impulse response function (IRF) of the setup. The green line is a walking average and the red line a fit of the data. **(A, B)**: the data was fitted with a double exponential decay. **(C, D)**: the data was fitted with a triple exponential decay. The graphs show that the triple exponential decay function fits better the fastest part of the emission curve.

TABLE 3 | Parameters of the double and triple exponential used, convolved with the IRF, to fit the data from the TCSPC measurements with a 2 × 2 × 3 mm^3 BaF_2 pixel from Proteus and Epic. Here τ_r is the rise-time, τ_{dn} the decay times, and R_n (n = 1, 2, 3) their corresponding abundances.

	τ_r (ps)	τ_{d1} (ns)	R_1 (%)	τ_{d2} (ns)	R_2 (%)	τ_{d3} (ns)	R_3 (%)	$\chi^2 \pm 0.0036$
Double exponential								
Proteus	0 ± 3	548 ± 5	94.0	0.606 ± 0.06	6.0	—	—	1.029
Epic	0 ± 3	686 ± 7	93.7	0.616 ± 0.06	6.3	—	—	1.008
Filter 240–395 nm + proteus	0 ± 3	640 ± 6	97.7	0.585 ± 0.06	2.3	—	—	1.004
Filter 250 nm + proteus	0 ± 3	542 ± 5	98.8	0.565 ± 0.06	1.3	—	—	1.010
Triple exponential								
Proteus	0 ± 3	551 ± 6	93.8	0.713 ± 0.07	5.3	0.057 ± 0.03	0.9	1.016
Epic	0 ± 3	689 ± 7	93.7	0.747 ± 0.07	5.4	0.078 ± 0.04	1.0	1.005
Filter 240–395 nm + proteus	0 ± 3	641 ± 6	97.6	0.786 ± 0.08	1.9	0.170 ± 0.09	0.5	1.002

emission abundance is slightly reduced (0.94–0.92) by the presence of the three coupling compounds, yet this reduction is not significant when compared with the air measurement. This is consistent with the transmission measurements of the greases, which show very little absorption in this wavelength region.

3.4. CTR Measurements

3.4.1. Measurements With Air Coupling

Figure 7 shows the CTR measurements with Proteus and Epic crystals. The obtained CTR values are 98 ± 5 ps FWHM for the Epic crystal and 94 ± 5 ps FWHM for the Proteus crystal. It can be concluded that with the given SiPM, the crystals of both producers perform the same within the limitations of the experimental setup. Therefore, the observed higher total light output from Proteus seems to be fully compensated by its higher absorption rate below 270 nm, resulting finally in an extracted amount of fast photons comparable to that of the Epic crystal. To put these numbers into context with commonly used bright and fast inorganic scintillators, such as LYSO:Ce of the same length with the same SiPM, the CTR was measured with such a scintillator and showed to produce a CTR of 140 ps FWHM, see also **Figure 7**. This CTR of 140 ps

TABLE 4 | Parameters of the double exponential fit, convolved with the IRF, used to describe the data from the TCSPC measurements with a $2 \times 2 \times 3$ mm^3 BaF_2 pixel from Proteus, using various optical coupling media and filters in front of the hybrid PMT. Here τ_r is the rise-time, τ_{dn} the decay times, and R_n (n = 1, 2, 3) their corresponding abundances.

	τ_r (ps)	τ_{d1} (ns)	R_1 (%)	τ_{d2} (ns)	R_2 (%)	$\chi^2 \pm 0.0036$
Proteus air	0 ± 3	548 ± 5	94.0	0.606 ± 0.06	6.0	1.029
Proteus viscasil	0 ± 3	615 ± 6	94.3	0.613 ± 0.06	5.7	1.050
Proteus glycerine	0 ± 3	623 ± 6	94.4	0.601 ± 0.06	5.6	1.031
Proteus dow corning	0 ± 3	612 ± 6	94.5	0.596 ± 0.06	5.5	1.039

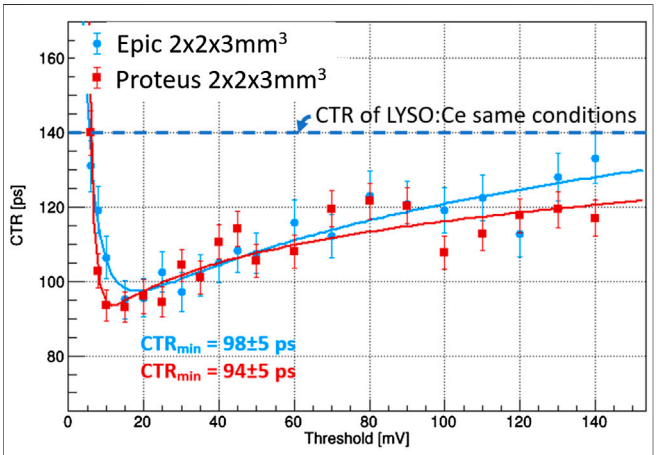

FIGURE 7 | CTR measurements of $2 \times 2 \times 3$ mm^3 BaF_2 pixels from Epic and Proteus, air coupled to a S13370-CN SiPM from Hamamatsu, operated at 61 V. For both fits of the data, the minimum value is written in the corresponding color.

TABLE 5 | CTR measurements of $2 \times 2 \times 3$ mm^3 BaF_2 pixels from Epic and Proteus, coupled to a S13370-CN of Hamamatsu, using various optical couplings.

	Bias	Air	Dow Corning	Glycerine	Viscasil
Epic	@ 60 V	104 ± 6	97.2 ± 5	91.9 ± 8	84.0 ± 4
Proteus	@ 60 V	102 ± 4	99.3 ± 4	105.9 ± 6	99.9 ± 5
Epic	@ 61 V	97.6 ± 5	93.6 ± 5	93.0 ± 8[a]	77.6 ± 4
Proteus	@ 61 V	93.6 ± 4	93.9 ± 4	106 ± 6[a]	87.4 ± 4

[a]*Measurement at a bias voltage of 60.8 V, since 61 V showed a excessive noise in this configuration.*

has to be seen in light of a more favorable PDE of the SiPM at the LYSO:Ce wavelength (26%) compared to that at the BaF_2 wavelength (~15%). Despite its more beneficial PDE, the air-coupled LYSO:Ce crystal cannot compete with the BaF_2 one. However under totally different conditions, when it is glued with Meltmount to its specifically developed SiPM (HPK S13360), the LYSO:Ce crystal reaches a coincidence time resolution of 86 ± 2 ps FWHM [37], only slightly better than its air-mounted competitor BaF_2.

3.4.2. Measurements With Optical Coupling

The results of the CTR measurements with the selected greases are summarized in **Table 5**. The SiPM bias used for comparing the different greases in terms of their CTR was 60 V. These results are also visualized in **Figure 8**. The operating voltage was then further increased to 61 V to assess the limits of the SiPM for highest CTR performance.

Figure 8 shows that, within the statistical limits, the CTR of the Proteus crystal shows no improvement no matter what grease is chosen. Only when pushing the bias voltage to 61 V, Viscasil together with the Proteus crystal shows a slight improvement in CTR, as can been seen in **Table 5**.

Unlike the Proteus crystal, whose CTR seems to be largely insensitive to any of the applied coupling agents, the Epic's CTR visibly benefits from these greases, with Viscasil being the best of all, allowing even a CTR of as high as 78 ± 4 ps FWHM when the SiPM bias is pushed to 61 V.

4. DISCUSSION

In this work, several characterizations have been performed to analyze and better understand the time resolution of BaF_2, using crystals produced by Epic Crystals and Proteus together with VUV SiPMs manufactured by Hamamatsu.

Transmission measurements show that, compared to Epic, crystals from Proteus absorb more light below ~270 nm, meaning that predominantly cross-luminescence light is being absorbed. This will have a negative effect on the CTR. Furthermore, as to the three coupling compounds Viscasil, Dow Corning and glycerine, they have been shown to be almost completely transparent down to 220 nm, before they begin to slightly absorb light below that. Among the three, glycerine in fact appeared as the most transparent as it transmits better below 220 nm than the others.

Light output measurements show Proteus having a consistently higher light output than Epic, on average by a factor of 1.15. This is to be seen in contrast to the transmission measurements, where the Proteus crystal was found to absorb more light occurring only in the wavelength range of the fast emission. The light output measurements, on the other hand, are dominated by the more abundant slow STE emission in the crystal, since its light yield is about 7–8 times higher than that from the fast cross-luminescence [22]. This leads to the conclusion that for Proteus at least the amount of extracted STE emission is higher than for Epic. However, considering the higher absorption of Proteus below 270 nm, this does not necessarily mean that the amount of extracted fast cross-luminescence light from Proteus is also a factor 1.15 higher than for Epic.

The outcome of TCSPC measurements shows that the emission kinetics of the Epic and Proteus crystals are the same, so are the abundances of the cross-luminescence emission. This was a priori not expected given the transmission measurements on the one hand, which showed a higher absorption in the cross-luminescence region for Proteus, and the light output measurements on the other hand,

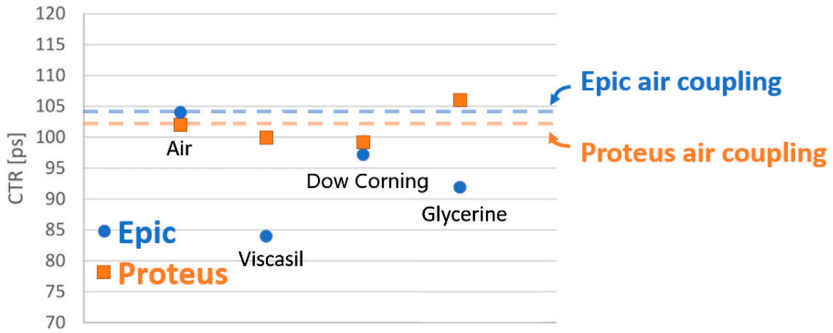

FIGURE 8 | Minima of CTR measurements (equals highest resolution) of $2 \times 2 \times 3\,mm^3$ BaF_2 pixels from Epic and Proteus, coupled to a S13370-CN of Hamamatsu, using various optical coupling media. Measurements were taken at a bias of 60 V.

showing a higher total light extraction for Proteus. This offset is probably due to the limited quantum efficiency at short wavelengths of the used HPK-100-07 hybrid PMT, making it less sensitive in the region where the Proteus crystal shows a higher absorption than Epic.

Furthermore, a very fast decay component, with a decay-time of ~0.1 ns has been observed, with an estimated abundance of 1%. This very fast emission was newly discovered by our group [10], its origin still being under investigation. Measurements with filters have demonstrated that the majority of its emission lies below 240 nm. Considering the limitations of the HPM-100-07 hybrid PMT in the setup, the abundance of this emission is most probably underestimated. From the TCSPC measurements one can derive that all the tested greases slightly, by 6–8%, absorb light in the region of the cross-luminescence emission.

As to coincidence time resolution, of prime interest in this study, both Epic and Proteus crystals produced comparable results of 94 ± 4 and 98 ± 5 ps FWHM, respectively, both with air coupling. This situation however changed when optical coupling greases were used to transfer the light from the crystal to the photodetector. Unlike the Proteus crystal, whose CTR seems to be largely insensitive to any of the coupling greases, the Epic's CTR visibly benefits from the optical coupling agents, with Viscasil being the best of all. With this compound, the CTR could even be improved to 78 ± 4 ps FWHM when pushing the SiPM bias voltage to 61 V. In general the difference in CTR performance between Epic and Proteus can be explained by the higher light absorption of the Proteus crystal below 270 nm.

However, despite the beneficial effects of the optical coupling greases on the global detection performance, their physical contact with the unprotected SiPM surface can lead to unexpected effects such as those observed here in the case of glycerine. Although being chemically inert and chosen for that purpose, glycerine systematically led to an increase in the SiPM's dark current, with its obvious negative effects on the CTR.

The scintillators used for the investigation in this article are short 3 mm long pixels. As the main purpose of this paper was to assess the timing potential of cross-luminescence in BaF_2 detected with newly developed deep-UV sensitive SiPMs, tests were made with short crystals in order to be comparable with similar measurements done for other materials, e.g., LYSO:Ce. The advantage of short crystals is that detrimental effects such as absorption and scattering in the crystal, more likely present in longer crystals, play a secondary role, which allows to better understand the CTR limits. In detectors for PET and HEP applications larger crystals, between 15 and 30 mm depending on the scintillator, are commonly used. Therefore, the next step in the investigation of cross-luminescence in BaF_2 for ultrafast timing applications is to explore the performance of longer crystals in order to further prove the competitiveness of BaF_2 with state-of-the-art scintillators, e.g., 20 mm LYSO:Ce pixel coupled to a Hamamatsu SiPMs with its 135 ps CTR performance [37].

In summary, this work has shown that, already with existing technologies, BaF_2 and a commercial Hamamatsu silicon photodetector produce a coincidence time resolution of as high as 94 ± 4 ps FWHM with air coupling and even 78 ± 4 ps FWHM when Viscasil is chosen as optical coupling agent. Better understanding of the "very fast" 100 ps decay component might give a handle to develop ways to even further increase this time resolution.

If the photon detection efficiency of SiPMs working in the deep UV could be improved from the current 15% to values of 60% not an untypical value for SiPMs at larger wavelengths [10], this would have an immediate impact on the coincidence time resolution, ultimately enabling to reach a CTR of $\sqrt{15/60} \cdot 86$ ps = 43 ps FWHM. Another prospect is to increase the single photon time resolution of the VUV SiPMs to values of <100 ps and hence be able to increase the CTR by another ~10 ps [10], opening the door to a new regime in coincidence time resolution of as low as 30 ps CTR with relatively heavy inorganic scintillators.

DATA AVAILABILITY STATEMENT

All datasets presented in this study are included in the article.

AUTHOR CONTRIBUTIONS

RP, EA, and SG developed as a team the idea of using VUV SiPMs for cross-luminescence readout for ultrafast timing. SG designed the readout for the coincidence time resolution measurements. RP wrote the manuscript, perfomed measurements on the transmission, light yield, coincidence time resolution, and corresponding data analysis.

SG and RP performed TCSPC measurements and corresponding data analysis. SG and EA reviewed the manuscript.

FUNDING

This work was performed in the framework of the Crystal Clear Collaboration. It was sponsored by the German Federal Ministry of Education and Research in the framework of the Wolfgang Gentner Program (grant no. 05E15CHA).

ACKNOWLEDGMENTS

We would like to thank all the members of the Crystal Clear team at The European Organization for Nuclear Research (CERN) for their support.

REFERENCES

1. Huizenga J, Seifert S, Schreuder F, van Dam H, Dendooven P, Löhner H, et al. A fast preamplifier concept for sipm-based time-of-flight pet detectors. *Nucl Instrum Methods Phys Res Sect A Accel Spectrom Detect Assoc Equip* (2012) **695**:379–84. doi:10.1016/j.nima.2011.11.012
2. Gundacker S, Auffray E, Frisch B, Jarron P, Knapitsch A, Meyer T, et al. Time of flight positron emission tomography towards 100ps resolution with L(y)SO: an experimental and theoretical analysis. *J Inst* (2013) **8**:P07014. doi:10.1088/1748-0221/8/07/p07014
3. Derenzo SE, Choong WS, Moses WW. Fundamental limits of scintillation detector timing precision. *Phys Med Biol* (2014) **59**:3261–86. doi:10.1088/0031-9155/59/13/3261.
4. Brunner SE, Gruber L, Marton J, Suzuki K, Hirtl A. Studies on the cherenkov effect for improved time resolution of tof-pet. *IEEE Trans Nucl Sci* (2014) **61**: 443–7. doi:10.1109/tns.2013.2281667
5. Omelkov S, Nagirnyi V, Vasil'ev A, Kirm M. New features of hot intraband luminescence for fast timing. *J Lumin* (2016) **176**:309–17. doi:10.1016/j.jlumin.2016.03.039
6. Lecoq P. Pushing the limits in time-of-flight pet imaging. *IEEE Trans Radiat Plasma Med Sci* (2017) **1**:473–85. doi:10.1109/trpms.2017.2756674
7. Cates JW, Gundacker S, Auffray E, Lecoq P, Levin CS. Improved single photon time resolution for analog SiPMs with front end readout that reduces influence of electronic noise. *Phys Med Biol* (2018) **63**:185022. doi:10.1088/1361-6560/aadbcd
8. Gundacker S, Turtos RM, Auffray E, Paganoni M, Lecoq P. High-frequency SiPM readout advances measured coincidence time resolution limits in TOF-PET. *Phys Med Biol* (2019) **64**:055012. doi:10.1088/1361-6560/aafd52
9. Lecoq P, Morel C, Prior J, Visvikis D, Gundacker S, Auffray E, et al. Roadmap toward the 10 ps time-of-flight pet challenge. *Phys Med Biol* (2020) [Epub ahead of print]. doi:10.1088/1361-6560/ab9500
10. Gundacker S, Turtos RM, Kratochwil N, Pots RH, Paganoni M, Lecoq P, et al. Experimental time resolution limits of modern SiPMs and TOF-PET detectors exploring different scintillators and cherenkov emission. *Phys Med Biol.* (2019) **65**:025001. doi:10.1088/1361-6560/ab63b4
11. Farukhi MR, Swinehart CF. Barium fluoride as a gamma ray and charged particle detector. *IEEE Trans Nucl Sci* (1971) **18**:200–4. doi:10.1109/TNS.1971.4325864
12. Ershov NN, Zakharov NG, Rodnyi PA. Spectral-kinetic study of the intrinsic-luminescence characteristics of a fluorite-type crystal. *Optic Spectrosc* (1982) **53**:51–4.
13. Andriessen J, Dorenbos P, Eijk CV. Electronic structure and transition probabilities in pure and Ce3+doped BaF2, an explorative study. *Mol Phys* (1991) **74**:535–46. doi:10.1080/00268979100102401
14. Laval M, Moszyński M, Allemand R, Cormoreche E, Guinet P, Odru R, et al. Barium fluoride—inorganic scintillator for subnanosecond timing. *Nucl Instrum Methods Phys Res* (1983) **206**:169–76. doi:10.1016/0167-5087(83)91254-1
15. van Eijk CWE Cross-luminescence. *J Lumin* (1994) **60–1**:936–41. doi:10.1016/0022-2313(94)90316-6
16. Rodnyi PA. Core-to-valence transitions. In: *Physical processes in inorganic scintillators*. Chap. 3.3. Cleveland, OH: CRC Press LLC (1997) p. 111–29.
17. Rodnyi PA. Core–valence luminescence in scintillators. *Radiat Meas* (2004) **38**:343–52. doi:10.1016/j.radmeas.2003.11.003
18. Ikeda T, Kobayashi H, Ohmura Y, Nakamatsu H, Mukoyama T. Electronic structure of alkaline-earth fluorides studied by model clusters. ii. auger-free luminescence. *J Phys Soc Jpn* (1997) **66**:1079–87. doi:10.1143/JPSJ.66.1079
19. Lecoq P, Gektin A, Korzhik M. *Inorganic scintillators for detector systems. Physical principles and crystal engineering.* 2nd ed. Cham, Switzerland: Springer (2017)
20. Valbis YA, Rachko ZA, Yansons YL. Short-wave UV luminescence of BaF_2 crystals caused by crossover transitions. *Soviet J Exp Theor Phys Lett* (1985) **42**: 172.
21. Novotny R, Riess R, Hingmann R, Ströher H, Fischer R, Koch G, et al. Detection of hard photons with baf2 scintillators. *Nucl Instrum Methods Phys Res Sect A Accel Spectrom Detect Assoc Equip* (1987) **262**:340–6. doi:10.1016/0168-9002(87)90871-0
22. Dorenbos P, de Haas J, Visser R, Eijk CWV, Hollander R. Absolute light yield measurements on baf/sub 2/ crystals and the quantum efficiency of several photomultiplier tubes. *IEEE Trans Nucl Sci* (1993) **40**:424–30. doi:10.1109/23.256593
23. Zhu R-y. *A barium fluoride crystal calorimeter for the ssc.* Berlin, Germany: Springer (1991) p. 437–55. doi:10.1007/978-1-4615-3746-5_44
24. Kirm M, Lushchik A, Lushchik C, Nepomnyashikh AI, Savikhin F. Dependence of the efficiency of various emissions on excitation density in baf2 crystals. *Radiat Meas* (2001) **33**:515–9. doi:10.1016/s1350-4487(01)00044-0
25. Derenzo S. The quest for new radiation detector materials (2008). Available at: https://www-group.slac.stanford.edu/ais/publicDocs/presentation88.pdf
26. Li HH. Refractive index of alkaline earth halides and its wavelength and temperature derivatives. *J Phys Chem Ref Data* (1980) **9**:161–290. doi:10.1063/1.555616
27. Zhu RY. The next generation of crystal detectors. *J Phys Conf Ser* (2015) **587**: 012055. doi:10.1088/1742-6596/587/1/012055
28. Sarukura N, Nawata T, Ishibashi H, Ishii M, Fukuda T. Czochralski growth of oxides and fluorides. In: P Rudolph, editor *Handbook of crystal growth*. 2nd ed. Chap. 4. Boston, MA: Elsevier (2015) p. 131–68.Google Scholar
29 Bell Z. Scintillation counters. In: *Handbook of particle detection and imaging.* Chap. 15. Berlin, Germany: Springer-Verlag (2012) p. 349–75.
30. Jansons JL, Krumins VJ, Rachko ZA, Valbis JA. Luminescence due to radiative transitions between valence band and upper core band in ionic crystals (crossluminescence). *Phys Status Solidi B* (1987) **144**:835–44. doi:10.1002/pssb.2221440244
31. Klamra W, Lindblad T, Moszyński M, Norlin L. Properties of optical greases for BaF_2 scintillators. *Nucl Instrum Methods Phys Res Sect A Accel Spectrom Detect Assoc Equip* (1987) **254**:85–7. doi:10.1016/0168-9002(87)90486-4
32. Jamil A, Ziegler T, Hufschmidt P, Li G, Lupin-Jimenez L, Michel T, et al. Vuv-sensitive silicon photomultipliers for xenon scintillation light detection in nexo. *IEEE Trans Nucl Sci* (2018) **65**:2823–33. doi:10.1109/TNS.2018.2875668
33. Gallina G, Giampa P, Retière F, Kroeger J, Zhang G, Ward M, et al. Characterization of the hamamatsu vuv4 mppcs for nexo. *Nucl Instrum Methods Phys Res Sect A Accel Spectrom Detect Assoc Equip* (2019) **940**: 371–9. doi:10.1016/j.nima.2019.05.096
34. Zhu R-y. On quality requirements to the barium fluoride crystals. *Nucl Instrum Methods Phys Res Sect A Accel Spectrom Detect Assoc Equip* (1994) **340**:442–57. doi:10.1016/0168-9002(94)90125-2
35. Gola A, Acerbi F, Capasso M, Marcante M, Mazzi A, Paternoster G, et al. Nuv-sensitive silicon photomultiplier technologies developed

at fondazione bruno kessler. *Sensors* (2019) **19**:308. doi:10.3390/s19020308

36. Gundacker S, Knapitsch A, Auffray E, Jarron P, Meyer T, Lecoq P. Time resolution deterioration with increasing crystal length in a tof-pet system. *Nucl Instrum Methods Phys Res Sect A Accel Spectrom Detect Assoc Equip* (2014) **737**:92–100. doi:10.1016/j.nima.2013.11.025
37. Gundacker S, Heering A. The silicon-photomultiplier: fundamentals and applications of a modern solid-state photon detector. *Phys Med Biol* (2020) **65:17TR01**. 10.1088/1361-6560/ab7b2d

Conflict of Interest: The authors declare that the research was conducted in the absence of any commercial or financial relationships that could be construed as a potential conflict of interest.